



Label-free multiplexed detection based on core-shell photonic barcodes integrated RCA

Dagan Zhang^{a,*}, Nan Zhang^a, Junqi Zhao^a, Xueqin Li^a, Feika Bian^a, Yi Zhang^{c,**},
Yizhi Ge^{b,***}, Zhiyang Li^{a,****}

^a Department of Clinical Laboratory, Institute of Translational Medicine, The Affiliated Drum Tower Hospital of Nanjing University Medical School, 210008, Nanjing, China

^b Department of Radiation Oncology, Jiangsu Cancer Hospital & Jiangsu Institute of Cancer Research & the Affiliated Cancer Hospital of Nanjing Medical University, Nanjing, Jiangsu, 210009, China

^c Department of Radiology, The Affiliated Drum Tower Hospital of Nanjing University Medical School, 210008, Nanjing, China

ARTICLE INFO

Keywords:

Barcode
Photonic crystal
Core-shell
RCA
Label-free

ABSTRACT

Multiplexed, rapid, and accurate virus quantification is of great value in biomedical detection. Herein, we proposed a label-free multiplexed virus screening quantitative biosensor based on color core-shell hydrogel photonic crystal (PhC) barcode integrated rolling circle amplification (RCA). The composite hydrogel shell was formed by acrylic acid and polyethylene glycol diacrylate, and the core silica photonic crystal was used as a detector. In addition, by adjusting the internal periodic structure, the PhC microcarrier was able to perform various color barcodes for the detection of different targets. Based on these excellent properties of the nano-composite barcode, the biosensor not only demonstrated the ability to rapidly and accurately detect SARS-CoV-2-N, SARS-CoV-2-S, and H1N1 simultaneously in one tube, but also converting the signal of target protein to nucleic acid signal based on DNA decorated antibody complex combine with the blocked primer and RCA strategy. As a result, the platform achieved highly sensitive multiplexed quantitative detection with a detection limit in the range of 0.30 pg/mL. In addition, the platform we developed was validated by clinical sample analysis with acceptable accuracy and high specificity, demonstrating the good potential applicability of the proposed detection method in clinical screening and diagnosis.

1. Introduction

The coronavirus disease 2019 (COVID-19), caused by severe acute respiratory syndrome coronavirus 2 (SARS-CoV-2), poses a serious threat to global public health and global activities, causing more than 70 million infections and 6.5 million deaths worldwide (Fenwick et al., 2021; Panpradist et al., 2021; Xun et al., 2021). It is worth noting that the relevant clinical symptoms (fever, cough, fatigue, or myalgia) caused by SARS-CoV-2 can easily be mistaken for the manifestations of influenza virus. Because the transmission mechanism (such as person-to-person transmission and aerosol or air droplets), and seasonal coincidence of the two respiratory diseases are similar (Yousefi et al., 2021). If it is not diagnosed promptly and accurately, the two respiratory

diseases may be misdiagnosed, and the simultaneous epidemic will not only increase the risk of epidemic prevention and control, but also in turn bring social panic and major challenges to the existing health system (Ning et al., 2021). Therefore, there is an urgent need for detection methods that can actively identify COVID-19 cases so that timely response can be given. Currently, the general detection methods of virus include real-time polymerase chain reaction (RT-PCR) by molecularly amplifying the virus RNA and immunoassay for virus-related proteins. Although RT-qPCR is a sensitive and accurate method, it faces some challenges in decentralized settings, such as expensive thermal cycler, and long readout time, skilled technical. Moreover, In addition, the RT-PCR method cannot distinguish between live or dead viruses, and amplification will produce false positive rates (Liu et al., 2023; Cheong

* Corresponding author.

** Corresponding author.

*** Corresponding author.

**** Corresponding author.

E-mail addresses: zhang.dagan@126.com (D. Zhang), zhang_yi0125@163.com (Y. Zhang), yzgoncology@163.com (Y. Ge), lizhiyang@nju.edu.cn (Z. Li).

<https://doi.org/10.1016/j.bios.2024.117037>

Received 7 August 2024; Received in revised form 20 November 2024; Accepted 4 December 2024

Available online 5 December 2024

0956-5663/© 2024 Elsevier B.V. All rights are reserved, including those for text and data mining, AI training, and similar technologies.

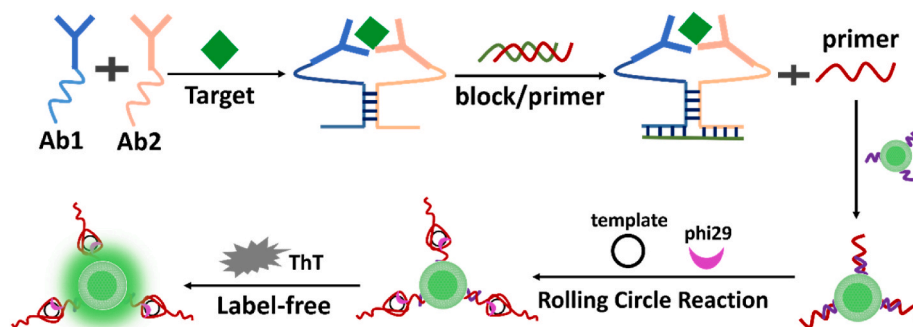


Fig. 1. Schematic process of label-free immunoassay platform based on RCA integrated core-shell structural color barcodes. (For interpretation of the references to color in this figure legend, the reader is referred to the Web version of this article.)

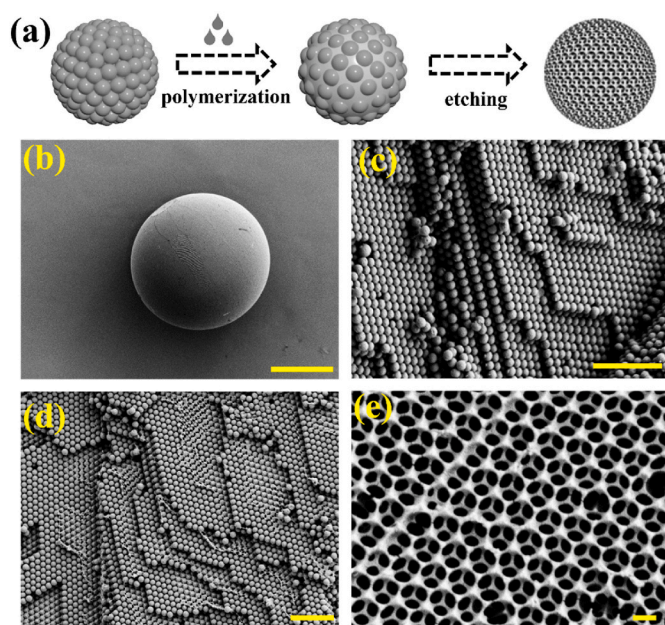


Fig. 2. (a) Schematic diagram of the fabrication of porous hydrogel-encapsulated PhC barcodes. (b) SEM images of spherical global morphology of the SiO₂ self-assembled barcode. (c) Microscopic characterization of bare surface morphology without hydrogel doping (d) Microscopic characterization of exposed surface morphology containing hydrogel permeated in the microsphere (e) The microscopic characterization of the shell surface obtained by etching silica. Scale bars of (b) are 100 μm, scale bars of (c and d) are 2.0 μm, scale bars of e are 0.2 μm.

et al., 2020; Wang et al., 2021). Immunoassay such as enzyme-linked immunosorbent assay (ELISA), and chemiluminescence immunoassay have attracted much attention due to their ability to quickly and specifically screen for certain viruses. Despite their great success, their limited sensitivity has hampered their application in timely diagnosis of diseases, because sometimes the initial viral load of the infection is low and difficult to detect (Bi et al., 2017). Therefore, to tackle these above-mentioned challenges, more and more attention was devoted to develop some signal amplification strategies boosting to accelerate the development of immunoassay, for example, the signal of immunoanalysis is converted into nucleic acid signal to achieve highly sensitive detection (Kazane et al., 2012). The current signal amplification methods contain loop-mediated isothermal amplification (LAMP), recombinase polymerase amplification (RPA), and rolling circle amplification (RCA). Among them, RCA describes a process of unidirectional nucleic acid replication that can rapidly synthesize multiple copies of circular molecules of DNA/RNA, which is widely used in limited

resources (Song et al., 2022; Chen et al., 2022b; Akter et al., 2024; Yang et al., 2024; Liang et al., 2024). However, these methods are often limited to the detection of a single virus and cannot achieve multi-target detection. In particular, the co-existence of COVID-19 and influenza puts tremendous pressure on society and medical personnel in practical application (Paria et al., 2022; Rafat et al., 2022). Therefore, the development of a new immunoassay strategy with high sensitivity and multi-target quantification is still worth looking forward to.

Here, we developed a novel multiplexed label-free platform based on core-shell photonic barcodes with integrated RCA signal amplification strategy. Various approaches have been designed to achieve multiplex analysis, including planar microarrays and suspension barcodes (Kim et al., 2017; Zayani et al., 2021; Zhang et al., 2020b). Among them, suspension barcodes have shown excellent performance with high flexibility, good reproducibility and fast reaction kinetics, which has attracted great interest in the biomedical field (Ackerman et al., 2020; Wang et al., 2019). In recent years, many researchers have devoted themselves to expanding the scope of suspension encoding strategies, including fluorescence, quantum dots and PhC barcodes. Among these barcodes, PhC barcodes are formed based on the self-assembly of periodic ordered nanostructures, which endow them with gorgeous structural colors and inherent characteristic reflection peaks. In addition, these unique barcodes have advantages such as stable encoding and no photobleaching properties. These properties make PhC particles a promising tool for multiplexed detection of various biomarkers without interference from fluorescence signals (Ji et al., 2019; Zhang et al., 2019; Luan et al., 2018; Liu et al., 2018; Cai et al., 2019; Yang et al., 2019). However, most detection methods based on photonic barcodes rely on fluorescent dye labeling, which has complex preparation processes and high costs, limiting their widespread application (Zhang et al., 2020a; Masterson et al., 2021; Hanpanich et al., 2020; Yan et al., 2023, 2024). In addition, the surface properties of traditional photonic barcode particles are poor and the probe immobilization efficiency is low (Chen et al., 2022a, 2024). Therefore, it is of great significance to develop novel barcode vectors for label-free multiplex virus detection.

In this paper, a novel label-free immunoassay platform that integrates core-shell PhC barcodes with RCA for highly sensitive multiplex virus detection is produced. Illustrated in Fig. 1, the platform employs a pair of DNA antibody conjugates to identify the target protein, leading to the formation of a proximity ligation complex Ab-1/target protein/Ab-2. This process triggers a strand displacement reaction (SDA), releasing the primer from the designed block/primer complex. Subsequently, the released primer hybridizes with the probe immobilized on the barcode, initiating RCA using C-rich circular DNA as a template to produce numerous G-quadruplexes and resulting in a robust fluorescent signal. As results, the signal of target protein was converted to nucleic acid signal. In addition, different PhC barcodes decorated with different probes can be used to achieve multiplex target determination. The results demonstrate that the composite immunoassay platform we developed is of great value for multiplex label-free detection of H1N1, SARS-

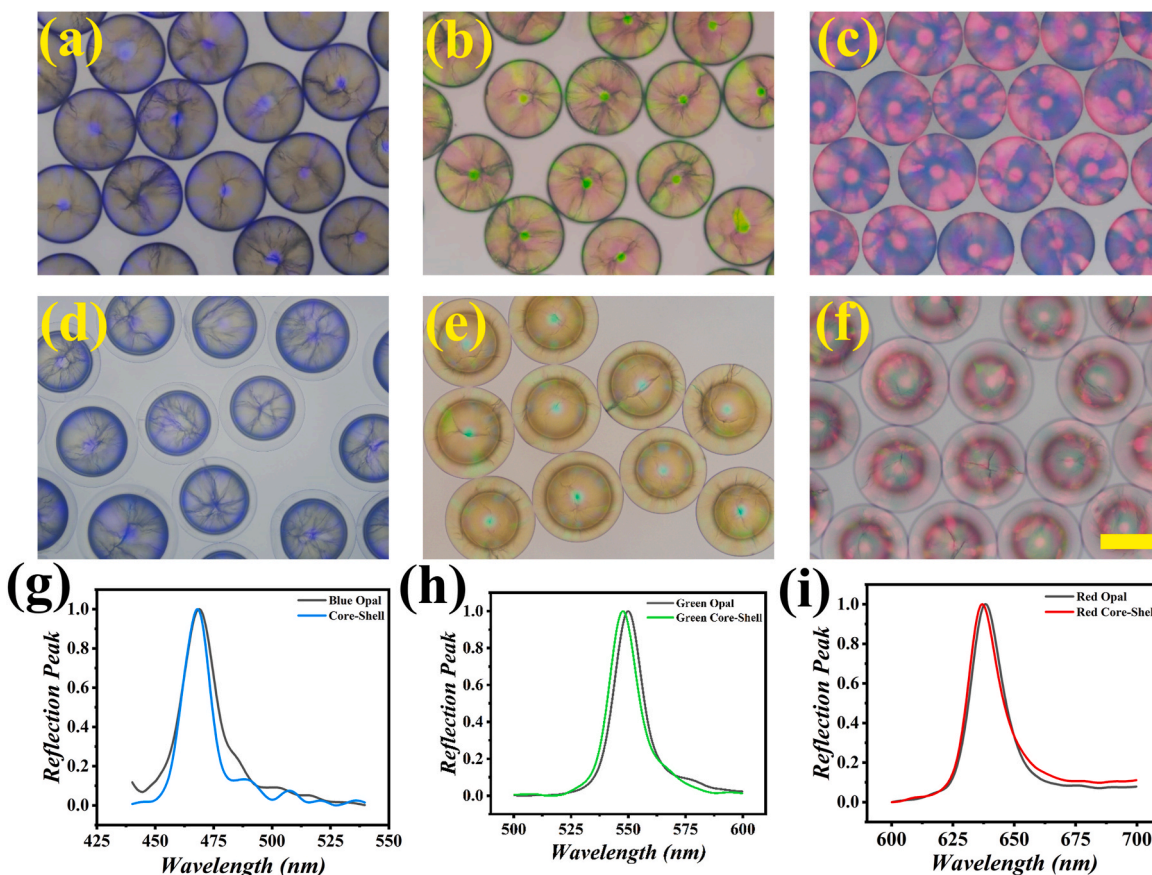


Fig. 3. (a–c) Optical images of three kinds of SiO₂ self-assembly microspheres. Scale bar represents 200 μ m; (d–f) Light microscope bright field image of different color core-shell barcode microspheres; (g–i) Reflection spectra comparison of three colors of SiO₂ self-assembly microspheres and that of core-shell barcode. (For interpretation of the references to color in this figure legend, the reader is referred to the Web version of this article.)

CoV-2-S, and SARS-CoV-2-N. Therefore, this innovative approach is expected to achieve multiplexed quantification of other pathogenic viruses and bacteria in many practical clinical applications.

2. Experimental methods

2.1. Preparation of core-shell SiO₂ self-assembly microspheres

The 20% Polyethylene glycol diacrylate (PEGDA) and 10% Acrylic acid (AA) serve as the hydrogel pregel solution and 1.0% 2-hydroxy-2-methylpropiophenone (HMPP) as the photoinitiator. The hydrogel pregel solution was filled into the dried PhC microspheres and kept for 2.0 h, followed by exposed under 365 nm ultraviolet for 30s to reinforce. Subsequently, the hydrogel microspheres were washed with ddH₂O to remove the surface impurity and followed by etched with 0.5% hydrofluoric acid (HF) for 30 min, and then a porous hydrogel-PhC shell microsphere was successfully obtained. Then, The gorgeous translucent beads are rinsed repeatedly with ultra-pure water.

2.2. Preparation of probe immobilization of PhC barcode platform

The hydrogel microspheres were treated with an activator such as 1-ethyl-3-(3-dimethylaminopropyl) carbodiimide (EDC), and N-hydroxy succinimide (NHS) buffer solution for 0.5 h and activated the carboxyl group on AA of microcarriers, and then were washed with Phosphate-buffered saline (PBS). These microspheres were covalent bond with the amino group of nucleic acid probes at 37 °C for 2.0 h and then blocked with BSA for 30 min. The different barcode microspheres were mixed with the corresponding target nucleic acid probes.

2.3. Antibodies decorated with DNA initiators

First, 100 μ L 0.5 mg/mL of anti-SARS-COV-2-N paired antibody (named as Ab-1/Ab-2) were incubated with the 2:1 M ratio of EDC and NHS for 60 min. Next, the 100 μ L DNA initiators (100 μ M) react with Ab-1/Ab-2 for 12 h at 4.0 °C, unbound nucleic acid initiator chains are removed by ultrafiltration. Finally, the obtained paired DNA-antibodies complex were stored in –20 °C for further use. Meanwhile, anti-SARS-COV-2-S, anti-H1N1 antibody labelled with DNA initiators by similar method.

2.4. Preparation of circular DNA

First, the primer (10 μ M) and the G-padlock (10 μ M) were added into 10 mM PBS (pH 7.4), which was reacted at 95 °C for 5 min, then slowly cooled to room temperature. Subsequent, a splint R ligase (25 U/ μ L) and the ligation buffer were incubated with the aforementioned complex for 2.0 h at 25 °C. Finally, the Exo III (100 U/ μ L) and CutSmart buffer were mixed with the ligation product at 37 °C for 2.0 h to get the complete circular DNA, and the termination reaction at 65 °C for 20 min. The obtained products were stored at –20 °C for further use.

2.5. Multiplex label-free detection

For multiplex label-free detection, three kinds of different probes were fixed on the hydrogel core-shell color beads, respectively. First, the different DNA decorated paired antibodies were mixed with three kinds of virus protein in range from 1.0 pg/mL–100 pg/mL for 0.5 h at 37 °C in the same tube. Next, three kinds of the probes decorated color beads, phi29 and the prepared circular DNA, the RCA reaction buffer, ThT were

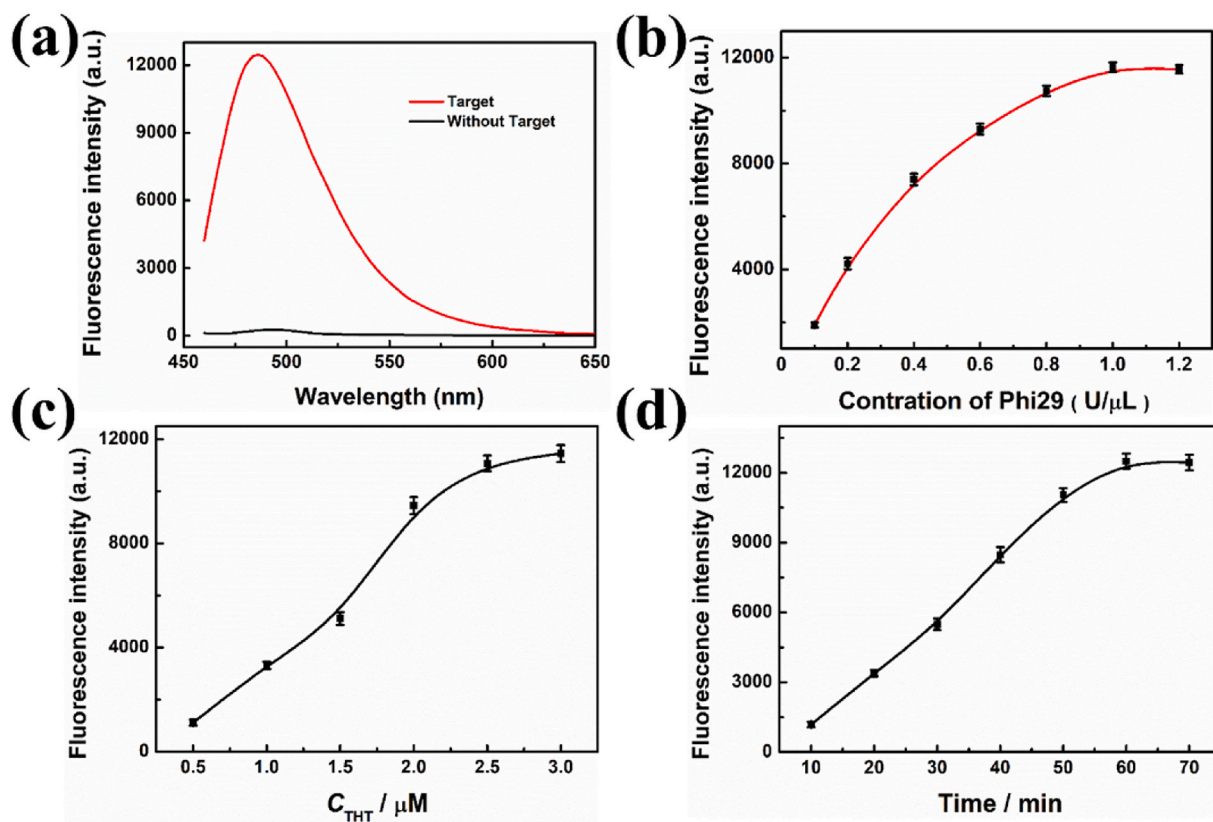


Fig. 4. (a) The fluorescence comparison in the presence or absence of target. (b) The fluorescence comparison by phi29 concentration (c) The fluorescence intensity comparison under different ThT concentration. (d) The optimization of the amplification time.

added into the mixture for 1.0 h at 37 °C. The fluorescence intensity is collected by fluorescence spectrometer, all experiments were conducted in three parallel groups.

3. Results and discussion

3.1. Principle of label-free detection biosensor

In this work, this label-free immunoassay platform utilized DNA decorated antibody complex combine with the blocked primer and RCA, which convert the target protein to the signal of nucleic acid. In the presence of the target protein, the DNA decorated antibody Ab1 and DNA decorated antibody Ab2 recognized the protein based on the specific combination of antigen and antibody forms the sandwich structure, which promotes the binding of two nucleic acid chains part complementing each other due to proximity effects. Thus, The unbound exposed portion of this complex could combine with the block/primer complex by a strand displacement reaction to release the primer. The released primer would hybridized with the probe immobilization on barcodes and then which triggered the RCA to produce a large amount of G4 duplicate sequences and the strong fluorescence signals with the help of ThT. Hence, the signal of target protein was converted to nucleic acid signal, the target protein concentration was measured by reading fluorescence intensities on core-shell structural color microsphere.

3.2. Construction of the porous PhC hydrogel microspheres

In a typical experiment, as shown in Fig. 2a. The porous PhC hydrogel microspheres were prepared by replicated silica nanoparticles assembly formed PhC templates. As shown in Fig. 2b and c. The PhC templates exhibited a hexagonal alignment nanostructure, which was were observed through scanning electron microscopy (SEM). The

prepared hydrogel solution was added into silica microspheres and entered the interconnected nanopores of the silica nanoparticles by capillary force. Subsequently, the pregel solution was polymerized under UV exposure after 30s to get the hydrogel hybrid microspheres, as shown in Fig. 2d. Finally, the hydrogel hybrid microspheres were selectively etching by 0.5% HF for 0.5 h to form the outer hydrogel shells with high order structure that show hexagonal symmetrical porous scaffolds (as shown in Fig. 2e) and meanwhile kept that of the cores of the hydrogel hybrid microspheres the same structures as that of PhC barcodes. Thus, the porous PhC hydrogel microcarriers were achieved.

The coding element is necessary for multiplex detection, PhC barcode was endowed with the characteristic reflectance spectra because of its the periodically ordered nanostructures. Besides, according to Bragg's equation: $\lambda = 1.633 d n_{\text{average}}$, the intrinsic unique reflectance spectra of the PhC barcodes were adjusted by the diameter of the ordered arrangement silica nanoparticles. Among the Bragg's equation, d refers to the distance of two neighboring nanoparticles, n_{average} refers to the average refractive index of the components of a substance. Owing to the porous PhC hydrogel microcarriers is copied from the PhC barcode template structure. Likewise, reflection peaks of hydrogel encapsulated barcodes also accord with Bragg's equation. The n_{average} of core-shell hydrogel barcode is determined by its components and proportion. Hence, the reflection peak is mainly related to the diameter of the hydrogel encapsulated barcodes. As shown in Fig. 3a–i, the SCCB templates possess vivid structural colors and a unique wavelength reflection spectrum at 470 nm, 550 nm and 635 nm, respectively. Besides, the reflection peak of the constructed core-shell encoding vector is almost the same as that of the template, and the change caused is negligible. More exciting, the core-shell barcodes still emerged stable and glaring colors even after hydrogel encapsulation, these results significate that the hydrogel encapsulated core-shell barcodes could serve as a multiplex detection platform.

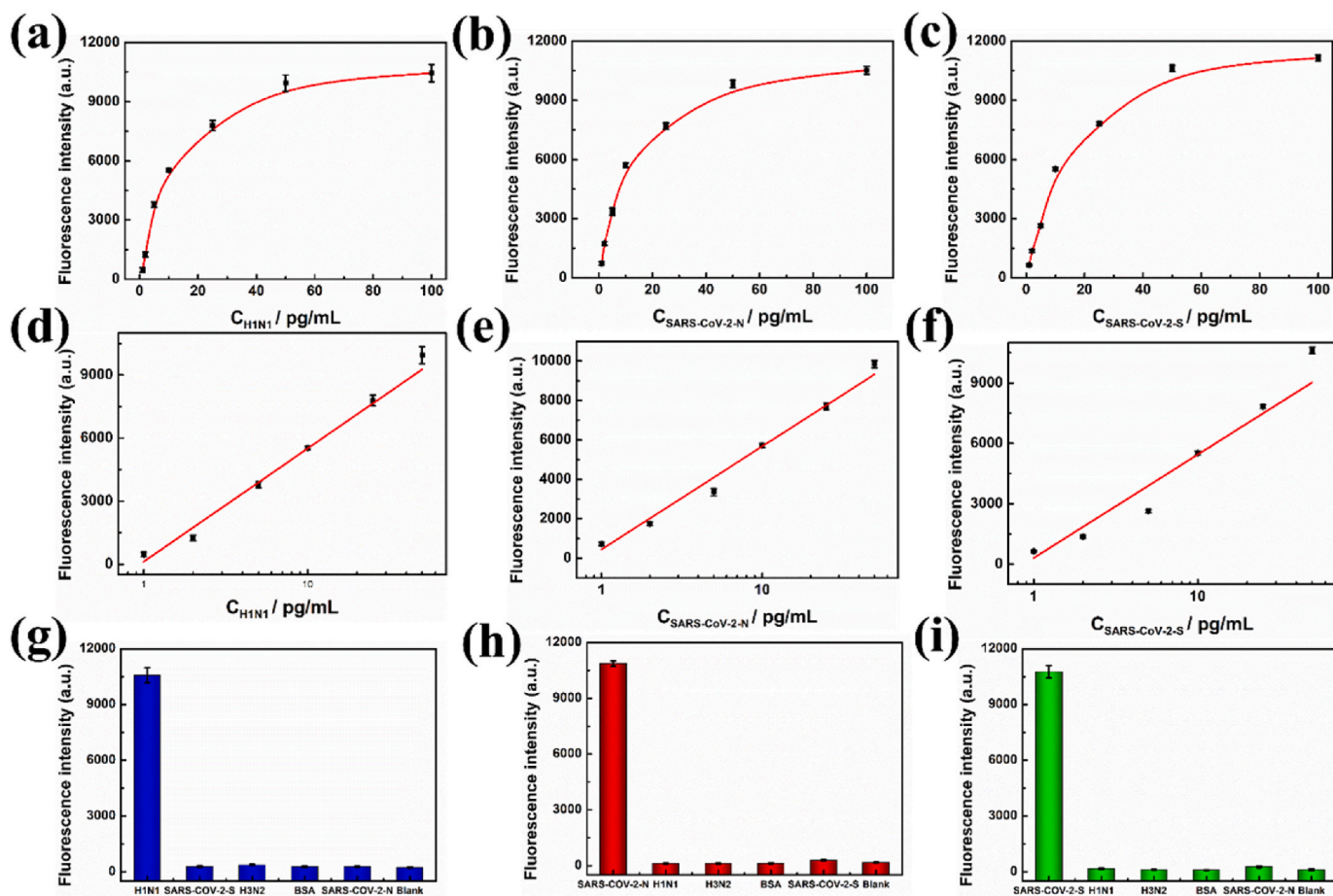


Fig. 5. (a–c) Fluorescence intensity statistics of H1N1 virus, SARS-CoV-2-N and SARS-CoV-2-S at different concentrations. (d–f) Linear analysis of fluorescence intensity of different virus concentrations of H1N1 virus, SARS-CoV-2-N and SARS-CoV-2-S. (g–i) The specificity evaluation of three targets in the presence of high concentrations of interfering substances. All tests were repeated 3 times.

3.3. Feasibility and optimization of detection conditions

To demonstrate the feasibility of this biosensors, the fluorescence intensity of this platform was compared. Once the target protein appeared, the paired DNA-antibodies Ab1 and Ab2 recognized the target protein to form the sandwich structure, which pulled in the distance of two nucleic acid chains fixed on the antibody and promoted the partial binding of the nucleic acid chains. The unbond part of the sandwich complex would combine with a designed block/primer complex by a strand displacement reaction to release the primer. And then initiator the following RCA to produce a strong fluorescent signal on core-shell microcarriers. As shown in Fig. 4a, the fluorescence intensity shows a sharp peak at 485 nm in the presence of target, however, that of without the target protein tended to horizontal line. The results showed that the method successfully converted protein detection into nucleic acid detection, and laid a foundation for the detection of low concentration protein biomarkers.

To better exploit the potentialities of the proposed method, some experimental conditions were optimized. In the RCA amplification, the concentration of phi29 enzyme is critical to the effect on reaction efficiency. Therefore, we investigated the effect of changes in enzyme concentration on the detection signal. As shown in Fig. 4b, the FL intensity generated by varying concentrations within 0–1.0 U exhibited an upward trend and there was no upward change even when the concentration was increased to 0.2 U. Hence, 1.0 U was selected as the optimal concentration of phi29 enzyme. Meanwhile, the concentration of ThT were evaluated, As shown in Fig. 4c, the FL intensity signal increased with the increasing concentration of ThT within 0.5–2.5 μ M

and tended to a maximum value and kept steady with another 0.5 μ M. Hence, the optimal concentration of ThT was 3.0 μ M. In addition, the reaction time of amplification determines the amount of product and thus influenced the FL intensity. As shown in Fig. 4d, The FL intensity reached the plateaued after incubation for 60 min, which was select as the optimal time for detection. In addition, the concentration of sodium ions has an important influence on the formation and stability of G4. At the same time, in order to better verify the detection of clinical samples, the sodium ion concentration in the human body is 90–140 mM, the verification was carried out in this concentration range. The final results showed that the fluorescence signal was relatively stable in the selected concentration range (Fig. S1).

To demonstrate the sensitivity of the proposed assay, the different concentrations of SARS-CoV-2-N in buffer was verified to this platform. As shown in Fig. 5, the signal intensity changes increasing with varying concentrations of SARS-CoV-2-N from 1.0 to 100 pg/mL (Fig. 5a). Furthermore, the proposed assay exhibited good linear response from SARS-CoV-2-N concentration from 1.0 to 50 pg/mL (Fig. 5d), and the limit of detection of this method was calculated to be 0.3 pg/mL, that calculated by the signal-to-noise ratio of 3. Besides, two other viruses such as H1N1 and SARS-CoV-2-S were also tested by this method with similar results (Fig. 5b, c, 5e and 5f), the above results demonstrated that the developed method presented a new multivariate amplification detection platform with similar sensitivity compared with the existing immuno-assay. Therefore, it is precisely because of the large amount of G4 produced in RCA amplification and the uniqueness of the encoding vector that the constructed platform has high sensitivity and selectivity. Compared with the conventional fluorescent labeling method, the

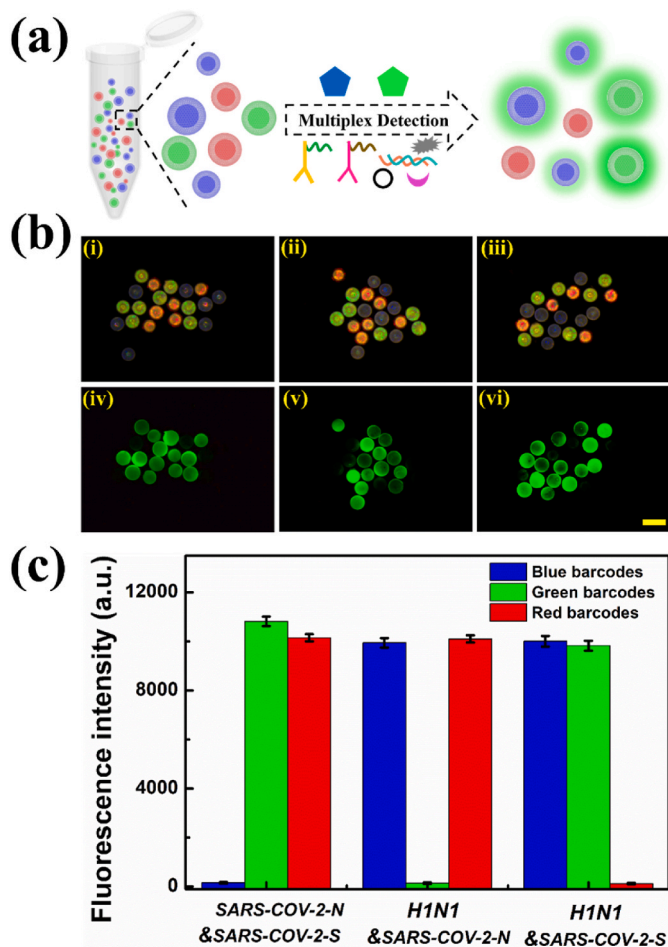


Fig. 6. (a) The schematic diagram of multiplex label-free virus detection; (b) Bright field microscopy and dark field fluorescence images of three kinds of core-shell color beads simultaneous incubating with two kinds of virus (c) Fluorescence intensity statistics of hydrogel core-shell color barcodes for simultaneous detection of two viruses. All tests were repeated 3 times. (For interpretation of the references to color in this figure legend, the reader is referred to the Web version of this article.)

results obtained by this method provide a new label-free detection platform with high accuracy and sensitivity.

We further investigated the specificity of this platform by measuring the signal intensity of interference target such as BSA, H3N2, and H1N1. The results in Fig. 5g displayed that even through the concentration of the interference (500 pg/mL) is 10 times the concentration of the target SARS-CoV-2-N (50 pg/mL). The intensity of the fluorescence signal measured by the interference object is almost the same as that of the blank control fluorescence signal, only when the target appears, the fluorescence signal will rise rapidly. Besides, the results in Fig. 5h and i showed that the specificity of SARS-CoV-2-S and H1N1 and was also explored and showed satisfactory results. Therefore, these results confirmed that our developed label-free multiplex platform based on core-shell barcode integrated RCA that boosting the potential for detecting viable pathogenic virus in complex sample.

3.4. Multiplexed label-free detection

The COVID-19 has brought a lot of economic losses and some complications to the public. In addition, the symptoms caused by conventional influenza viruses are basically similar to those caused by the SARS-CoV-2 coronavirus, which is easy to mislead the public in treatment. Therefore, it is essential to develop a novel method for immediate

intervention and effectively distinguish these virus. Therefore, we constructed a novel core-shell barcode combined with RCA signal amplification technology for the simultaneous label-free detection of the above three viruses, as shown in Fig. 6a. The corresponding probes of the three viruses were fixed on three color-coded microspheres. In the presence of the target virus, antibodies modified with nucleic acid DNA bind specifically to capture the virus and form a sandwich structure, thus encouraging the nucleic acid chains on the antibody to approach each other and hybridize. The unhybridized DNA segment binds to the block/primer complex and initiates SDA to release the primer chain. The released primer would bind to the nucleic acid probe on the microsphere and initiate RCA, producing a strong fluorescent signal on core-shell microcarriers. Moreover, to demonstrate the capability and accuracy of the developed method for multiplex detection, two viruses were added to the same tube for simultaneous detection. As shown in Fig. 6b and c, these results displayed that the excellent multiplex capability and high specificity of the proposed strategy for the target virus. Finally, this platform also evaluated successfully through three virus H1N1, SARS-CoV-2-N, and SARS-CoV-2-S simultaneous detection (Fig. S2). All of these above data highlighted that this method had the capacity to achieve label-free, multiplexed, highly sensitive and specific detection.

3.5. The clinical testing performance of the platform

Finally, the constructed platform was validated to gauge the potential application in real sample detection by incorporating three virus samples at known concentrations into throat swab samples collected by Department of Clinical Laboratory, The Affiliated Drum Tower Hospital. The obtained results displayed that the recoveries of three types of viruses in real samples ranged from 89.6 to 114.1% (Fig. S3). These satisfactory findings indicate that the method exhibits excellent accuracy, reliability, and sensitivity when applied to complex clinical samples. Additionally, a comparison between our developed method and a commercial ELISA method revealed comparable diagnostic efficiency (Fig. S4). In summary, we have proposed a novel and cost-effective label-free immunoassay for simultaneous detection of various pathogens in future in vitro diagnosis.

4. Conclusion

In summary, in this study, we proposed an innovative label-free immunoassay platform for multiplexed virus detection based on RCA integrated core-shell hydrogel PhC barcodes. The core-shell barcodes not only retains the colored structural color as the core layer for encoding detection, but also contains abundant probe binding sites in the shell structure. In the presence of corresponding target, the corresponding antibodies recognized the target protein to drive the series of signal amplification reaction and converted the protein detection to the nucleic acid detection, finally form lots of G4 duplicate sequences and fluorescence signal on barcodes. With these advanced advantages, the H1N1, SARS-CoV-2-N, SARS-CoV-2-S multiplexed label-free high-sensitivity detection could be relied, the limit of detection reached to 0.30 pg/mL. More importantly, the developed label-free platform was further validated in clinical samples, maintaining reliable results compared with the gold standard. Finally, our strategy demonstrates promising application prospects for multiplexed influenza virus detection in early clinical diagnosis.

CRediT authorship contribution statement

Dagan Zhang: Writing – review & editing, Writing – original draft, Conceptualization. **Nan Zhang:** Methodology. **Junqi Zhao:** Writing – original draft, Validation. **Xueqin Li:** Validation. **Feika Bian:** Validation. **Yi Zhang:** Writing – review & editing, Supervision. **Yizhi Ge:** Investigation. **Zhiyang Li:** Conceptualization.

Notes

The authors declare no competing financial interest.

Declaration of competing interest

We declare that we do not have any commercial or associative interest that represents a conflict of interest in connection with the work submitted.

Acknowledgements

This work was supported by the National Natural Science Foundation of China (82102511, 82102181), the Natural Science Foundation of Jiangsu (BK20210021, BK20210009), and the Research Project of Jiangsu Province Health Committee (M2021031), and Clinical Trials from the Affiliated Drum Tower Hospital, Medical School of Nanjing University (2024-LCYJ-MS-15). Nanjing Medical Science and Technique Development Foundation (YKK23068, JQX22002).

Appendix A. Supplementary data

Supplementary data to this article can be found online at <https://doi.org/10.1016/j.bios.2024.117037>.

Data availability

Data will be made available on request.

References

- Ackerman, C.M., Myhrvold, C., Thakku, S.G., Freije, C.A., Metsky, H.C., Yang, D.K., Ye, S. H., Boehm, C.K., Kosoko-Thoroddsen, T.F., Kehe, J., Nguyen, T.G., Carter, A., Kulesa, A., Barnes, J.R., Dugan, V.G., Hung, D.T., Blainey, P.C., Sabeti, P.C., 2020. Massively multiplexed nucleic acid detection with Cas13. *Nat.* 582 (7811), 277–282.
- Akter, J., Smith, W.J., Gebrewold, M., Kim, I., Simpson, S.L., Bivins, A., Ahmed, W., 2024. Evaluation of colorimetric RT-LAMP for screening of SARS-CoV-2 in untreated wastewater. *Sci. Total Environ.* 907, 167964.
- Bi, S., Yue, S., Zhang, S., 2017. Hybridization chain reaction: a versatile molecular tool for biosensing, bioimaging, and biomedicine. *Chem. Soc. Rev.* 46 (14), 4281–4298.
- Cai, L., Bian, F., Sun, L., Wang, H., Zhao, Y., 2019. Condensing-enriched magnetic photonic barcodes on superhydrophobic surface for ultrasensitive multiple detection. *Lab Chip* 19 (10), 1783–1789.
- Chen, H., Bian, F., Guo, J., Zhao, Y., 2022a. Aptamer-functionalized barcodes in herringbone microfluidics for multiple detection of exosomes. *Small Methods* 6 (6), 2200236.
- Chen, H., Bian, F., Luo, Z., Zhao, Y., 2024. Biomimetic anticoagulated porous particles with self-reporting structural colors. *Adv. Sci.*, 2400189.
- Chen, Y., Liu, F., Lee, L.P., 2022b. Quantitative and ultrasensitive in situ immunoassay technology for SARS-CoV-2 detection in saliva. *Sci. Adv.* 8 (21), eabn3481.
- Cheong, J., Yu, H., Lee, C.Y., Lee, J.U., Choi, H.J., Lee, J.H., Lee, H., Cheon, J., 2020. Fast detection of SARS-CoV-2 RNA via the integration of plasmonic thermocycling and fluorescence detection in a portable device. *Nat. Biomed. Eng.* 4 (12), 1159–1167.
- Fenwick, C., Turelli, P., Pellaton, C., Farina, A., Campos, J., Raclot, C., Pojer, F., Cagno, V., Nusslé, S.G., D'Acremont, V., 2021. A high-throughput cell- and virus-free assay shows reduced neutralization of SARS-CoV-2 variants by COVID-19 convalescent plasma. *Sci. Transl. Med.* 13 (605), eabi8452.
- Hanpanich, O., Saito, K., Shimada, N., Maruyama, A., 2020. One-step isothermal RNA detection with LNA-modified MNazymes chaperoned by cationic copolymer. *Biosens. Bioelectron.* 165, 112383.
- Ji, J., Lu, W., Zhu, Y., Jin, H., Yao, Y., Zhang, H., Zhao, Y., 2019. Porous hydrogel-encapsulated photonic barcodes for multiplex detection of cardiovascular biomarkers. *ACS Sens.* 4 (5), 1384–1390.
- Kazane, S.A., Sok, D., Cho, E.H., Uson, M.L., Kuhn, P., Schultz, P.G., Smider, V.V., 2012. Site-specific DNA-antibody conjugates for specific and sensitive immuno-PCR. *Proc. Natl. Acad. Sci. U.S.A.* 109 (10), 3731–3736.
- Kim, D., Kwon, H.J., Shin, K., Kim, J., Yoo, R.E., Choi, S.H., Soh, M., Kang, T., Han, S.I., Hyeon, T., 2017. Multiplexable wash-free immunoassay using colloidal assemblies of magnetic and photoluminescent nanoparticles. *ACS Nano* 11 (8), 8448–8455.
- Liang, P., Li, J., Pi, Z., Zhang, X., Yu, X., Lai, G., 2024. Hyperbranched RCA-mediated construction of a dendritic DNA nanostructure for ratiometric fluorescence biosensing. *Sens. Actuators B Chem.* 412, 135797.
- Liu, J., Chen, P., Hu, X., Huang, L., Geng, Z., Xu, H., Hu, W., Wang, L., Wu, P., Liu, G.L., 2023. An ultra-sensitive and specific nanoplasmonic-enhanced isothermal amplification platform for the ultrafast point-of-care testing of SARS-CoV-2. *Chem. Eng. J.* 451, 138822.
- Liu, P., Chen, J., Zhang, Z., Xie, Z., Du, X., Gu, Z., 2018. Bio-inspired robust non-iridescent structural color with self-adhesive amorphous colloidal particle arrays. *Nanoscale* 10 (8), 3673–3679.
- Luan, C., Wang, H., Han, Q., Ma, X., Zhang, D., Xu, Y., Chen, B., Li, M., Zhao, Y., 2018. Folic acid-functionalized hybrid photonic barcodes for capture and release of circulating tumor cells. *ACS Appl. Mater. Interfaces* 10 (25), 21206–21212.
- Masterson, A.N., Muhoberac, B.B., Gopinadhan, A., Wilde, D.J., Deiss, F.T., John, C.C., Sardar, R., 2021. Multiplexed and high-throughput label-free detection of RNA/spike protein/IgG/IgM biomarkers of SARS-CoV-2 infection utilizing nanoplasmonic biosensors. *Anal. Chem.* 93 (25), 8754–8763.
- Ning, B., Huang, Z., Youngquist, B.M., Scott, J.W., Niu, A., Bojanowski, C.M., Zvezdaryk, K.J., Saba, N.S., Fan, J., Yin, X.-M., 2021. Liposome-mediated detection of SARS-CoV-2 RNA-positive extracellular vesicles in plasma. *Nat. Nanotechnol.* 16 (9), 1039–1044.
- Panpradist, N., Kline, E.C., Atkinson, R.G., Roller, M., Wang, Q., Hull, I.T., Kotnik, J.H., Oreskovic, A.K., Bennett, C., Leon, D., 2021. Harmony COVID-19: a ready-to-use kit, low-cost detector, and smartphone app for point-of-care SARS-CoV-2 RNA detection. *Sci. Adv.* 7 (51), eabj1281.
- Paria, D., Kwok, K.S., Raj, P., Zheng, P., Gracias, D.H., Barman, I., 2022. Label-free spectroscopic SARS-CoV-2 detection on versatile nanoimprinted substrates. *Nano Lett.* 22 (9), 3620–3627.
- Rafat, N., Zhang, H., Rudge, J., Kim, Y.N., Peddireddy, S.P., Das, N., Sarkar, A., 2022. Enhanced enzymatically amplified metallization on nanostructured surfaces for multiplexed point-of-care electrical detection of COVID-19 biomarkers. *Small* 18 (49), 2203309.
- Song, M., Hong, S., Lee, L.P., 2022. Multiplexed ultrasensitive sample-to-answer RT-LAMP chip for the identification of SARS-CoV-2 and influenza viruses. *Adv. Mater.*, 2207138.
- Wang, C., Liu, M., Wang, Z., Li, S., Deng, Y., He, N., 2021. Point-of-care diagnostics for infectious diseases: from methods to devices. *Nano Today* 37, 101092.
- Wang, Y., Shang, L., Bian, F., Zhang, X., Wang, S., Zhou, M., Zhao, Y., 2019. Hollow colloid assembled photonic crystal clusters as suspension barcodes for multiplex bioassays. *Small* 15 (13), 1900056.
- Xun, G., Lane, S.T., Petrov, V.A., Pepa, B.E., Zhao, H., 2021. A rapid, accurate, scalable, and portable testing system for COVID-19 diagnosis. *Nat. Commun.* 12 (1), 2905.
- Yan, J., Bhadane, R., Ran, M., Ma, X., Li, Y., Zheng, D., Salo-Ahen, O.M.H., Zhang, H., 2024. Development of Aptamer-DNAzyme based metal-nucleic acid frameworks for gastric cancer therapy. *Nat. Commun.* 15 (1), 3684.
- Yan, J., Ma, X., Liang, D., Ran, M., Zheng, D., Chen, X., Zhou, S., Sun, W., Shen, X., Zhang, H., 2023. An autocatalytic multicomponent DNAzyme nanomachine for tumor-specific photothermal therapy sensitization in pancreatic cancer. *Nat. Commun.* 14 (1), 6905.
- Yang, M., Liu, Y., Jiang, X., 2019. Barcoded point-of-care bioassays. *Chem. Soc. Rev.* 48 (3), 850–884.
- Yang, Y., Bu, S., Zhang, X., Duan, Q., Meng, H., Hao, Z., He, X., Wan, J., 2024. Influenza virus detection using an electrochemical biosensor based on DSN and RCA. *Microchem. J.* 199, 109998.
- Yousefi, H., Mahmud, A., Chang, D., Das, J., Gomis, S., Chen, J.B., Wang, H., Been, T., Yip, L., Coomes, E., 2021. Detection of SARS-CoV-2 viral particles using direct, reagent-free electrochemical sensing. *J. Am. Chem. Soc.* 143 (4), 1722–1727.
- Zayani, R., Rezig, D., Fares, W., Marrakchi, M., Essafi, M., Raouafi, N., 2021. Multiplexed magnetofluorescent bioplatfrom for the sensitive detection of SARS-CoV-2 viral RNA without nucleic acid amplification. *Anal. Chem.* 93 (32), 11225–11232.
- Zhang, D., Cai, L., Bian, F., Kong, T., Zhao, Y., 2020a. Label-free quantifications of multiplexed mycotoxins by g-quadruplex based on photonic barcodes. *Anal. Chem.* 92 (4), 2891–2895.
- Zhang, D., Cai, L., Bian, F., Tan, H., Zhao, Y., 2020b. Multiplexed detection of tumor biomarkers utilizing immunohybridization Chain reaction integrated photonic barcodes. *Sens. Actuators B Chem.* 321, 128535.
- Zhang, X., Chen, G., Bian, F., Cai, L., Zhao, Y., 2019. Encoded microneedle arrays for detection of skin interstitial fluid biomarkers. *Adv. Mater.* 31 (37), e1902825.